International Journal of Ambient Energy

ISSN: 0143-0750 (Print) 2162-8246 (Online) Journal homepage: www.tandfonline.com/journals/taen20

Optimisation of single-slope solar still performance using response surface methodology

T. G. Sakthivel, R. Manikandan, S. Purushothaman, N. Punitha, T. Gopalakrishnan, C. Gnanavel & V. S. Shaisundaram

To cite this article: T. G. Sakthivel, R. Manikandan, S. Purushothaman, N. Punitha, T. Gopalakrishnan, C. Gnanavel & V. S. Shaisundaram (2026) Optimisation of single-slope solar still performance using response surface methodology, International Journal of Ambient Energy, 47:1, 2711313, DOI: 10.1080/01430750.2026.2711313

To link to this article: https://doi.org/10.1080/01430750.2026.2711313

Published online: 11 Aug 2026.

INTERNATIONAL JOURNAL OF AMBIENT ENERGY
2026, VOL. 47, NO. 1, 2711313
https://doi.org/10.1080/01430750.2026.2711313

Taylor & Francis by informa

Check for updates

Optimisation of single-slope solar still performance using response surface methodology

T. G. Sakthivel [a], R. Manikandan [a], S. Purushothaman [b], N. Punitha [c], T. Gopalakrishnan [d], C. Gnanavel [d] and V. S. Shaisundaram [d]

[a]Department of Mechanical Engineering, Saveetha School of Engineering, Saveetha Institute of Medical and Technical Sciences (SIMATS), Saveetha University, Chennai, Tamil Nadu, India; [b]School of Engineering and Technology, Jaipur National University, Jaipur, India; [c]Department of Physics, St. Joseph's College of Engineering, Chennai, India; [d]Department of Mechanical Engineering, Vels Institute of Science Technology & Advanced Studies, Chennai, India

ABSTRACT

The increasing demand for low-cost and energy-efficient desalination systems has intensified interest in solar distillation technologies. The optimisation of a single-slope solar still with respect to ambient temperature, wall lining thickness, solar radiation, and wind velocity was carried out in this study using Response Surface Methodology (RSM) based on the Central Composite Design (CCD). A total of thirty experiments were carried out to assess the influence and interactions of the process parameters on freshwater productivity. The highest temperature of the basin, glass, water and vapour was 68.5°C, 63.25°C, 68.0°C and 66.5°C respectively. The productivity of the freshwater in the lined basin was also improved: from 1260 mL/day for the unlined basin to 2230 mL/day and 2330 mL/day for the 4 mm and 8 mm wall lining thicknesses, respectively, with a productivity increase of 77% and 85% respectively. The developed quadratic regression model exhibited excellent predictive accuracy, with an R^2 of 0.9926. The optimum conditions resulted in a production of 2330 mL/day under a 1.96% prediction error. The distilled water met the WHO drinking water standards, which is an indicator of the ability of the proposed system to produce freshwater in a sustainable manner.

ARTICLE HISTORY
Received 7 March 2026
Accepted 24 July 2026

KEYWORDS
Solar desalination; renewable water purification; solar still efficiency; thermal performance optimisation; sustainable water distillation; solar energy water treatment

Nomenclature

Heat Transfer Terms

Q_b	Convection heat transfer from basin liner to water, W
Q_{bot}	Conductive heat transfer from basin liner to ambient through bottom side, W
Q_{bw}	Conduction heat transfer from inner to outer side through back wall, W
Q_{cg}	Convection heat transfer from glass to ambient, W
Q_{cw}	Convection heat transfer from water to glass, W
Q_d	Rate of heat energy of distilled output, W
Q_{ew}	Evaporative heat transfer from water to glass, W
Q_{rg}	Radiation heat transfer from glass to ambient, W
Q_{rw}	Radiation heat transfer from water to glass, W
Q_{sw}	Conduction heat transfer from inner to outer side through side wall, W
Q_{sww}	Conductive heat transfer from the inside still to outside through water contact vertical sides, W

Temperatures

T_a	Ambient temperature, °C
T_b	Basin liner temperature, °C
T_{bwi}	Inside back wall temperature, °C
T_{bwo}	Outside back wall temperature, °C
T_g	Glass temperature, °C
T_{swi}	Inside side wall temperature, °C
T_{swo}	Outside side sidewall temperature, °C
T_v	Vapour temperature, °C
T_w	Water temperature, °C

Abbreviations

ANOVA	Analysis of variance
BBD	Box Behnken design
cm^2	Square centimetre
cm^3	Cubic centimetre
DF	Degree of freedom
L	Litre
m	Metre
ml	Millilitre
mm	Millimetre
MS	Mean square
$MS_{regression}$	Mean squares regression
$MS_{residual}$	Mean square residual
RSM	Response surface methodology
R^2	Coefficient of determination
$R^2{}_{adj}$	Adjusted R-squared
SS	Sum of squares

1. Introduction

Freshwater scarcity is a growing problem around the world caused by the growing demand of humans, industries, and a decline in natural water sources. The conventional desalination

CONTACT R. Manikandan mani131990@gmail.com; C. Gnanavel gnanavelmech1986@gmail.com; V. S. Shaisundaram saiswastik23@gmail.com

technologies such as reverse osmosis (Qasim et al. 2019), electrodialysis (Lauer et al. 2019), membrane distillation (Liu et al. 2019) and multi-stage flash distillation (Hanshik et al. 2016) are energy intensive and infrastructure dependent, and are unavailable in remote and resource-constrained areas. Passive solar distillation utilising solar energy to vaporise saline or brackish water and to recover the distillate as potable water provides an autonomous and low-maintenance, low-cost water production alternative (Durkaieswaran and Murugavel 2015) for decentralised water production. The single-slope solar still is the most investigated type of passive still, due to its ease of construction, lack of moving components and for being suitable for small-scale development (Hussen et al. 2023). The energy efficiency is not as high as in more advanced multi-effect or active systems, though this can be significantly enhanced by systematic optimisation of the operating and design parameters of the system at low cost, and so freshwater productivity can be considerably enhanced (Nafey et al. 2000).

Various amounts of research have been conducted in order to improve the productivity of a single-slope solar still by modifying the basin absorber surface with a wick or with porous material. The main mechanism is capillary-assisted wetting, where a hygroscopic material lines the bottom of the basin, which pulls water up into the structure, thereby increasing the wetted evaporative surface area over the flat basin floor. In earlier research, several strategies have been shown to increase the productivity and thermal efficiency of solar stills by changing the geometry, using energy storage materials, using nanomaterials and by optimisation methods. The experimental studies conducted on the stepped solar stills combined with reflectors and fan-assisted air flow system have shown substantial improvement in the production of freshwater in arid climatic conditions due to increased evaporation and condensation processes (Yuvaperiyasamy 2025). Ahmed (Ahmed 2016) tested five different types of wicks (jute, cotton, felt, palm fibre and black cotton cloth) and concluded that the best distillate output was obtained using a black cotton cloth wick because of its better capillary action and absorptivity towards the Sun's rays. Srivastava and Agrawal (Srivastava and Agrawal 2013) discussed that the distillate productivity using dark cotton fabric fins in the basin was about 15% more as compared to a conventional still. Bhargava et al. (Bhargva and Yadav 2019) have found that bamboo cotton attained the highest DY of 3.03 L/m^2 with 34.5% efficiency, among the cotton, wool, jute and bamboo cotton wicks. In single-slope stills, Suraparaju et al. (Suraparaju and Natarajan 2020) found that natural fibres (cotton) have greater thermal performance advantage. Most importantly, each of these studies changed the type of wick material in use, but kept the thickness of the wick constant. The effect of systematically varying the thickness of a cotton cloth lining when optimising it together with climatic variables in a design framework based on statistics has not been reported earlier. This is a gap that is specific and fixable in the literature.

The climatic and design parameters govern the performance of a single-slope solar still. Solar radiation has been recognised generally as the main energy input: Morse et al. (Garg 1975) analytically proved that solar insolation was the most important factor determining still productivity, and this result was confirmed in all experimental studies. Nafey et al. (Nafey et al. 2000) proved that ambient temperature is a significant influence on basin water temperature and the evaporation rate, along with solar radiation. Wind velocity influences the glass cover temperature through two mechanisms. First, the external airflow lowers the glass cover temperature, thereby enhancing the condensation rate. Second, increased wind velocity intensifies convective heat loss from the glass surface to the surrounding environment. Keshtkar et al. (Keshtkar, Eslami, and Jafarpur 2020) investigated the effects of wind speed from 1 to 6 m/s and glass thickness from 4 to 2 mm on productivity and efficiency, respectively, by performing a transient CFD study, and found that productivity increased by 14.4% with wind speed increased from 1 to 6 m/s, and efficiency increased by 3.5% with glass thickness decreased from 4 to 2 mm and the optimal water depth and glass inclination were 2 cm and local latitude angle, respectively. Kabeel et al. (Kabeel et al. 2019) proved that the productivity of tubular still is maximum for lower water depth (less than 3 cm) because of less thermal mass. El Hafid et al. (El Hafid et al. 2023) investigated the performance of a cascade still with varying thickness of glass cover (3, 5 and 7 mm) and concluded that the thinner the glass cover, the higher the temperature of the absorber plate and the hourly efficiency. As mentioned, the individual parametric studies are known, but there has been no previous study that has optimised all of the parameters (ambient temperature, wall lining thickness, solar radiation and wind velocity) within one framework of experimental design for one single-slope still.

Response Surface Methodology (RSM) with Central Composite Design (CCD) serves as a systematic and statistically effective approach for optimisation of multiple continuous variables and modelling of their interaction. To optimise the productivity of a modified single-slope still, Haitham, Jamel, and Ihab (2020) used RSM to generate a quadratic model by varying water depth, cover inclination and saline water flow rate without considering the wall insulation and lining thickness. The model had an R^2 of 0.9903 and an F-value of 330.13. Again, Rejeb et al. (Rejeb et al. 2021) used the RSM to study the behaviour of a solar still by changing water depth (d), ambient temperature (T) and solar irradiance (E) and obtained a good predictive model ($R^2 > 0.98$), but they did not take into account wall material and lining thickness as an optimisation variable. Abed et al. (Abed et al. 2022) investigated the performance of stills with one slope under different solar conditions for the impact of chemical dyes. All these RSM studies concluded that the CCD framework is well suited for solar still optimisation, but in all the investigations, the wall lining thickness was not included in the set of variables, as it has been reported that it affects the heat retained in the basin and the surface area of evaporation (Bhargva and Yadav 2019; Srivastava and Agrawal 2013; Suraparaju and Natarajan 2020). One major drawback in previous RSM-based solar still research is the lack of information on the thickness of the wall. The present work is intended to fill this void.

In the same way, optimisation studies of single-slope solar stills with various thermal energy storage materials like paraffin wax, basalt stone, blue metal stone and kanche marbles observed that the amount of heat retained and distillate obtained increased remarkably with the use of phase change material (Yuvaperiyasamy et al. 2025). Other investigations on pyramid solar stills showed that decreasing the water depth of the basin increases the evaporation rate and the freshwater productivity, and paraffin wax showed that it has better thermal storage performance than other sensible heat storages (Yuvaperiyasamy, Senthilkumar, and Deepanraj 2025). Besides, the nano TiO_2-based modified pyramid solar stills with Taguchi optimisation were found to be very effective in enhancing the desalination efficiency and thermal performance when the nanomaterial was incorporated into the solar stills and the operating conditions were optimised (Senthilkumar, Yuvaperiyasamy, and Deepanraj 2024). Concentrated research has been reported and focused on the modification of geometry of solar stills, use of thermal energy storage materials and nanoparticle enhancement, but little has been reported on the simultaneous effect of the nano CuO-coated floated absorbers on both the desalination productivity and water quality characteristics. Thus, the present experimental study aims at improving the productivity of the desalination process and potable water produced in a solar still by introducing nano CuO-coated floated absorber.

A critical review of the earlier studies reveals that response surface methodology (RSM) coupled with a central composite design (CCD) has been widely applied for the optimisation of solar stills using climatic parameters such as solar radiation, ambient temperature, wind velocity, and water depth. However, no study has considered wall lining thickness as an optimisation parameter in combination with these operating variables. Besides, the effect of variable-thickness 8 mm cotton cloth lining is not systematically investigated by a multi-variable statistical method. Thus, the present study fills this gap by using a four-variable Central Composite Design with 30 experimental runs to achieve optimum ambient temperature (30–40°C), wall cotton cloth lining thickness (0–8 mm), solar radiation (300–900 W/m^2) and wind velocity (1–2 m/s) for a single-slope solar still to maximise freshwater productivity. The study also intends to use ANOVA and response surface analysis to determine the individual and interaction effect of these parameters, validate a quadratic regression model used to predict freshwater productivity within the experimental range, determine the optimum operating condition within the experimental range and evaluate the economic feasibility of the optimised configuration using a cost-per-litre analysis. To the best of the authors' knowledge, this combined experimental-statistical-economic approach applied to wall-thickness variation in a single-slope solar still has not been previously reported.

2. Materials and methods

The experiments were carried out from March to May (summer season) on the roof-top of the Department of Mechanical Engineering in Saveetha School of Engineering, Chennai, India (13.07°N, 80.12°E). The solar still was placed with glass cover on the south side at a constant inclination angle of 10° to the horizontal, similar to the local latitude as well as recommended by Keshtkar et al. (Keshtkar, Eslami, and Jafarpur 2020). Saline water with a total dissolved solids (TDS) concentration of 3500 ± 50 ppm (prepared by dissolving a measured mass of NaCl in tap water, verified with a calibrated TDS metre) was used as the feed water in all experiments. The water level in the basin was checked daily with the graduated steel ruler attached to the back wall of the basin and recorded to the first millimetre before each run and any daily test was carried out, and was set to 30 mm (around 15 litres for the 0.5 m^2 basin area). Testing took place every day for 8 h (from 09:00 to 17:00 IST), and hourly readings were taken of basin temperature, glass temperature, water temperature, vapour temperature, solar irradiance, wind velocity and cumulative distillate volume.

The solar still is made up of a glass cover, brackish water, an absorber plate, and an insulating layer (thermocol, 25.4 mm thick) placed beneath the basin to minimise downward heat loss, as illustrated in Figure 1. The collection plate captures the energy and passes the heat to the saltwater by means of convection. In order to limit energy lost through the absorber plate, an insulating barrier is put behind the solar still. Heat is transferred to the water through the process of convection to the absorber plate. As a result of heat transfer from the absorber plate by conduction and convection, combined with direct absorption of solar radiation by the water mass, the basin water temperature rises progressively, driving evaporation from the water surface at temperatures well below the boiling point. The basin surface is coated with black pigment and aligned along its elongated axis in a specific direction to maximise the absorption of solar radiation. The upper covering of the solar still, which is inclined at an angle of 10 degrees, is made of a conventional transparent window with a thickness of 4 millimetres. This glass covering has been encased within a wooden frame and securely sealed with rubber, which functions as an anti-air leakage mechanism. C-clamps are employed to create a seal between the glass cover and the body of the still to prevent the escape of vapour.

The entirety of the still is housed within a robust wooden frame with a thickness of 12 millimetres, with an insulating layer of thermocol (expanded polystyrene) of 25.4 mm thickness positioned between the solar still body and the outer wooden frame to reduce lateral and bottom heat losses. Temperature measurements were made using twelve K-type thermocouples connected to a 12-point digital indicator. The four optimisation parameters, namely ambient temperature, wall lining thickness, solar radiation and wind velocity, were chosen because of the ease of experimentation and their effect on solar still productivity. Four-variable Central Composite Design was used, with 30 experimental runs found to be appropriate in the experimental resources available. The water depth, glass thickness, and the glass inclination were kept constant in the study at 30 mm, 4 mm and 10° respectively, which were optimum values reported in previous studies and standard design considerations. The thickness of the lining material of the wall was selected as the main novel parameter, as it has not been considered in the previous solar still optimisation studies based on RSM. Other parameters such as water depth and glass inclination should also be tested in a broader optimisation range to be included in further studies. The term wall lining thickness throughout this study refers exclusively to the thickness of the cotton cloth lining applied to the inner basin walls: 0 mm (no lining), 4 mm (single layer), and 8 mm (double layer). The structural wooden wall (12 mm) and the thermocol insulation behind it (25.4 mm) remain constant across all experimental runs and are independent of this variable (Tables 1 and 2).

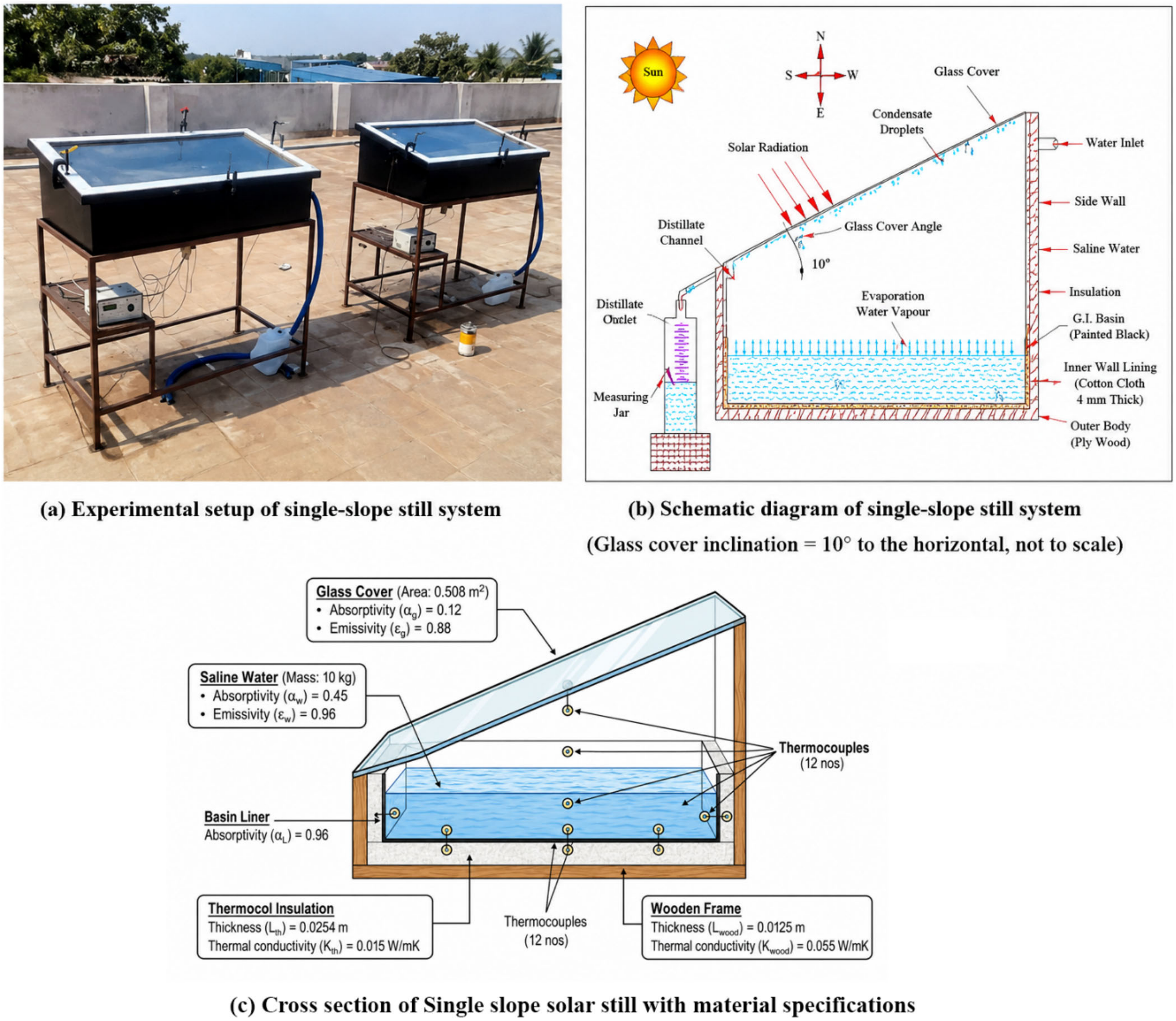

Figure 1. Experimental setup, schematic illustration, and cross-sectional configuration of the single-slope solar still with wall lining thickness arrangement and material specifications.

Table 1. Geometrical specifications of single slope solar stills.

S. No.	Dimensions	Measurements
1	Length	1 m
2	Width	0.5 m
3	Glass cover inclination	10°
4	Number of glasses	1
5	Thickness of glass cover	0.004 m

Table 2. Basic properties of single slope solar still.

S. No.	Specification	Dimension
1	Absorptivity of basin liner (αb)	0.96
2	Glass area (*Ag*)	0.508 m^2
3	An emissivity of glass (ϵg)	0.88
4	Absorptivity of glass (αg)	0.12
5	Thermocouples	12 nos
6	Absorptivity of water (αw)	0.45
7	The emissivity of water (ϵw)	0.96
8	Mass of saline water	10 kg
9	Thickness of thermocol (*Lth*)	0.0254
10	Thermal conductivity of thermocol (*Kth*)	0.015 W/mK
11	Thickness of wood (*Lwood*)	0.0125
12	Thermal conductivity of wood (*Kwood*)	0.055 W/mK

2.1. Measurement uncertainty evaluation

Calibration was carried out using thermocouples, a solarimeter, and an anemometer, as shown in Figure 2. Different instruments were used to measure the operating parameters of the solar still system. Wind velocity was measured using a digital anemometer, while solar radiation was recorded using a solarimeter. Temperature variations during the desalination process were monitored using twelve K-type thermocouples connected to a digital thermometer with an accuracy of ±1°C and a measurement range of 0–99.9°C. The solarimeter had a measurement range of 0–2000 W/m^2 with a least count of 1 W/m^2. Distilled water output was measured using a cylindrical measuring jar with a minimum reading of 1 mL. Ambient air velocity was measured using

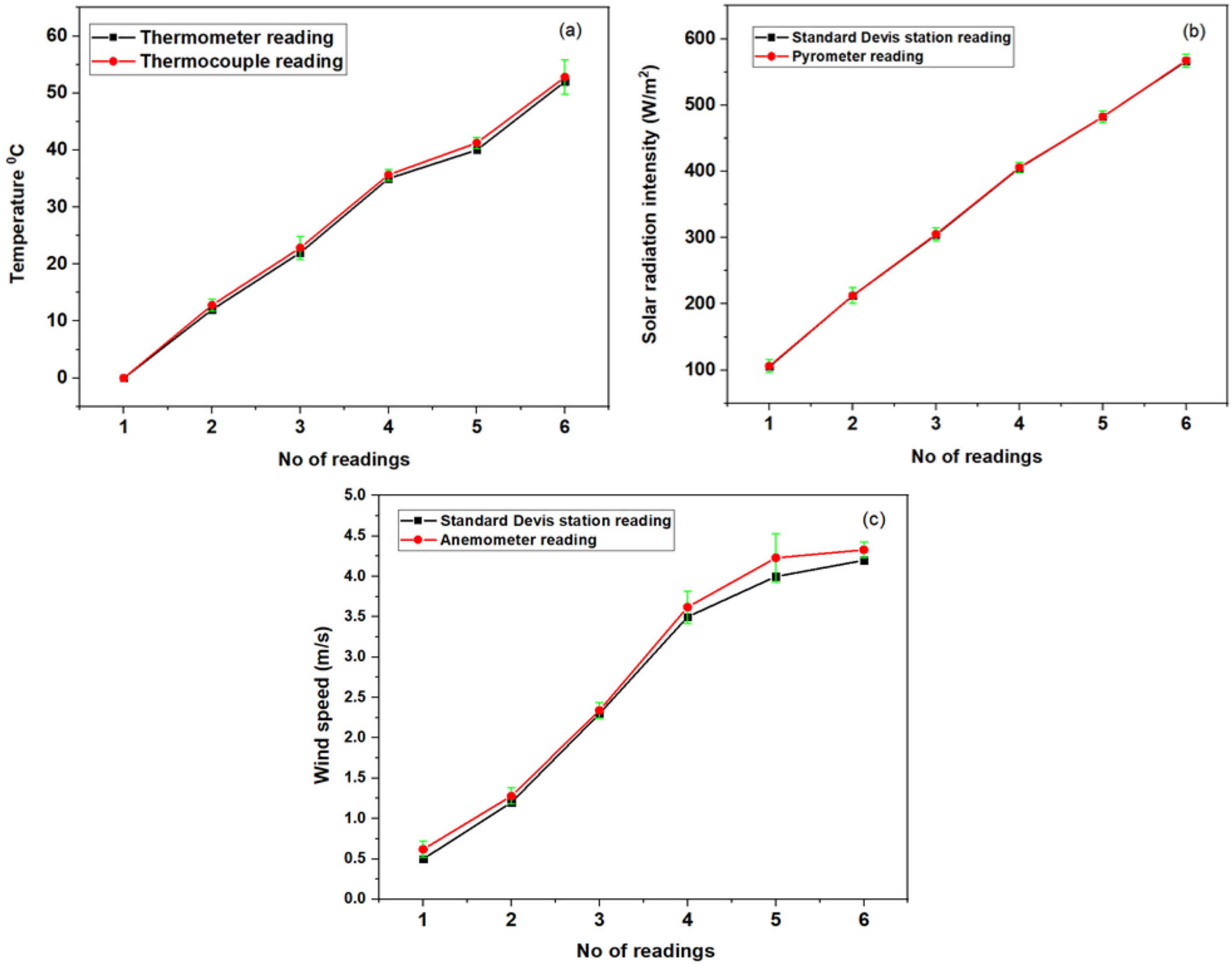

Figure 2. Calibration analysis (a) thermocouple (b) pyrometer (c) anemometer.

an electronic anemometer with a minimum detectable value of 0.1 m/s. A 300 mm steel ruler with a least count of 0.5 mm was fixed along the basin wall to measure the water level inside the solar still.

Uncertainty in Thermal Efficiency (η):

$$\delta\eta/\eta = \sqrt{[(\delta m/m)^2 + (\delta I/I)^2 + (\delta A/A)^2]}$$

where: δm = ±1 mL = ±0.001 kg (at typical m = 2.33 kg/day ÷ 8 h = 0.29 kg/h per interval) → δm/m = ±0.34%

$$\delta I = \pm 1\ W/m^2\ (at\ typical\ I \approx 600\ W/m^2) \rightarrow \delta I/I \approx \pm 0.17\%$$

δA = negligible (basin dimensions measured with steel rule, ±0.5 mm on 1 m → δA/A ≈ ±0.1%)

$$\therefore \delta\eta/\eta = \sqrt{(0.34^2 + 0.17^2 + 0.1^2)} \approx \pm 0.40\%$$

Overall uncertainty in thermal efficiency: ≤ ±1.2% (including all systematic errors).

The root-sum-of-squares (RSS) propagation method was adopted to perform a formal uncertainty analysis. Finally, the overall uncertainty in thermal efficiency was estimated as ±1.2% and the uncertainty in the measurement of the daily productivity as ±1 mL (±0.04% at the maximum productivity of 2330 mL/day). The uncertainty of temperature measurement is ±1°C for each thermocouple and the differential (Tw – Tg) is ±1.41°C. Wind velocity uncertainty is ±0.1 m/s, which equals ±5–10% over the range of 1–2 m/s. The range of measurement uncertainties is within the accepted limits of the passive solar still experimental studies. The 5 CCD centre-point replicates all had a standard deviation of ±9.4 mL/day, demonstrating the repeatability of the measurement.

3. Mathematical formulation for thermal efficiency and productivity

The total productivity of single-slope solar still is calculated from the following Equation (Yuvaperiyasamy et al. 2025):

$$p_d = \sum_{1}^{d.w.h} ph \tag{1}$$

where P is the total productivity (L/m²/day), mi is the mass of distillate collected during each time interval I (in litres), A is the area of the solar still (in square metres), and n is the number of time intervals during the day.

Fresh water enhancement of solar still:

$$p_{enh} = \frac{(pd)_p - (pd)_c}{(pd)_c} \quad (2)$$

where, p_{enh}-Percentage of enhancement, $(pd)_p$-Proposed solar still, $(pd)_c$-Conventional solar still.

The thermal efficiency of traditional solar distillation systems is determined using the methodologies proposed by Suraparaju and Natarajan (2021) and Kabeel and Abdelgaied (2016).

Total thermal efficiency: (Yuvaperiyasamy et al. 2025)

$$\eta_{energy} = \frac{\sum m_w * L}{(A * \sum I * 3600)} \quad (3)$$

where η_{th} is the total thermal efficiency of the solar still, m is the mass of distilled water collected (kg), I is the solar irradiance (W/m^2), A is the area of the solar still (m^2).

where L can be calculated

$$L = 2.4935*10^6*[1 - (9.4779*10^{-4}T_w + 1.3132*10^{-7}*{T_w}^2 - 4.794*10^{-9}*{T_w}^3] \quad (4)$$

4. Response surface methodology (RSM)

RSM entails the amalgamation of mathematical and statistical methodologies, rendering it invaluable in the facilitation of process development, optimisation, and improvement. A notable attribute of RSM lies in its ability to establish a precise model that relates the response and independent variables, achieved through the utilisation of the analysis of variance method (ANOVA).

Regression polynomial equation in quadratic form can be expressed as follows (Rejeb et al. 2021)

$$y = \beta_0 + \sum_{i-1}^{n} \beta_i x_i + \sum_{i=1}^{n} \beta_{ii} {x_i}^2 + \sum_{i=1}^{n-1} \sum_{j-i+1}^{n} \beta_{ij} x_i x_j \quad (5)$$

The response variable is represented by Y, and the independent variables by X_1 and X_2. The regression coefficients include b_0 for the intercept, b_1 and b_2 for the linear terms, b_3 and b_4 for the quadratic functions, and b_5 for the interaction term.

The adequacy of the mathematical model is determined by the adjusted multiple determination coefficients and the normal multiple determination coefficients (Rejeb et al. 2021)

$$R^2 = 1 - \frac{SS_E}{SS_T} \quad (6)$$

Where, SSE-is the sum of squared errors, R^2 – determination coefficients, SST is the total sum of squares

$$SS_T = \sum_{i=1}^{n} ({y_i}^2) - \frac{\sum_{i=1}^{n} ({y_i}^2)}{n} \quad (7)$$

$$SS_E = \sum_{i=1}^{n} (y_i - \bar{y}_i)^2 (y_i, \bar{y}_i) – (observed\ and\ fitted\ values)$$

The adjusted multiple determination coefficient is (Rejeb et al. 2021)

$${R_{adj}}^2 = 1 - (1 - R^2)\frac{n-1}{n-p} \quad (8)$$

n is the number of observations, p is the number of predictors (including the intercept term).

The most common minimum design for fitting a 2nd-order (quadratic) model with 4 factors is the 30-run Central Composite Design, which has 14 model degrees of freedom and 15 residual degrees of freedom. The design is orthogonal, both in the factorial and axial parts, with less correlation between parameters. The PRESS statistic of cross-validation gives a Predicted R^2 of 0.9595, which is a direct confirmation of the good generalisation of the model, since it was tested with 30 training runs. The ratio of Adequate Precision was 34.98, which is nearly at the adequate precision threshold, and shows that the 30 sample runs had a signal-to-noise ratio of almost 9 times the adequate precision ratio. These statistics support the adequacy of the sample size for the quadratic model used in this study.

5. Results and discussion

5.1. Experimental results

Figure 3 illustrates the temperatures for both a standard and a modified single-slope solar still, including the basin (Tb), glass (Tg), water (Tw), and vapour (Tv). The experiments were conducted from 09:00 to 17:00 IST under clear to partially clear sky conditions (cloud cover $\leq$ 2 oktas), with solar irradiance ranging from 350 W/m^2 at 09:00 to a peak of 950 W/m^2 at solar noon, ambient temperature between 32°C and 40°C, and wind speed between 1.2 and 4.0 m/s as recorded by the calibrated solarimeter and anemometer. The highest temperature on the interior wall surfaces is recorded between 14:00 and 15:00, while the lowest temperature on the atmospheric side is noted between 16:00 and 17:00. Furthermore, it is apparent that from 12:00 onwards, the T_{bi} remains at its highest level until the completion of the experiments. Figure 4 compares the glass cover temperatures of the conventional and modified solar still configurations under different operating conditions. At 8:00, it was evident that there was no significant difference in the temperatures of the stills being observed. This can be attributed to the fact that the trials commenced at 8:00, and the measured temperatures closely aligned with the ambient temperature, which was consistent throughout the study. The temperature difference over the next hour indicates that the still with an 8 mm thickness had higher vapour and basin water temperatures compared to the other stills. The highest recorded temperatures for the basin (Tb), glass (Tg), water (Tw), and vapour (Tv) were 68.5°C, 63.25°C, 68°C, and 66.5°C, respectively. The recorded temperatures during the time interval of 10:00 to 16:00 exhibited the lowest values for the C.S. This observation signifies that all the presently suggested approaches for modification are effectively enhancing the operational efficiency of the conventional solar still. This assertion can be substantiated by comparing the rise in temperature across all parameters with the corresponding values for the C.S.

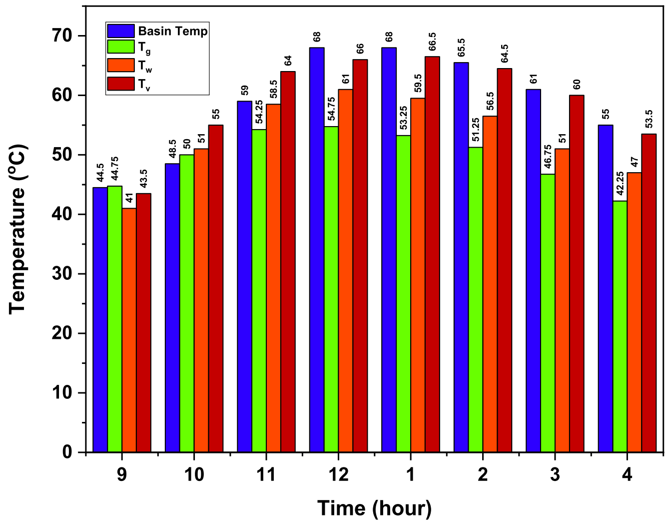

Figure 3. Temperature distribution (^{0}C) for Basin, T_g, T_w, T_v.

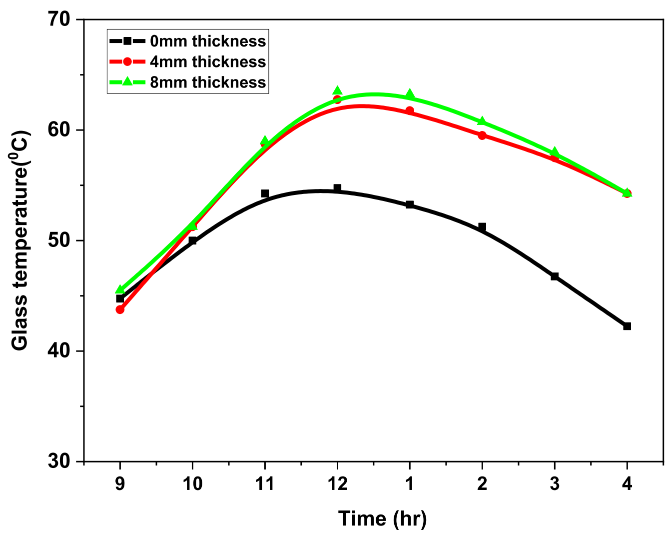

Figure 4. Comparison of glass temperatures in conventional and modified solar stills.

Two saturation mechanisms are responsible for the non-linear productivity response as a function of wall lining thickness; a large gain between thickness of 0 mm and 4 mm (from 1260 to 2230 mL/day) and a diminishing gain between 4 mm and 8 mm (from 2230 to 2330 mL/day). First, the 4 mm lining alone provides near complete wetting of the inner basin wall surface at the tested water depth; the layer in the 8 mm is only a small increment above the water line. Second, wall conduction heat loss accounts for a decreasing percentage of total still heat loss when a minimum wall lining thickness is achieved, and additional reduction of wall conduction heat loss is relatively small when compared to the dominating heat loss pathway, which is the glass-cover heat loss. The incremental cost of using 8 mm over 4 mm is around Rs. The productivity gain is about 30 L/year per additional person, which is a payback period of 1–2 years at current retail water prices, whereas 400–500 corresponds to the small portion (less than 5%) of the total system cost. The 8 mm configuration is thus maintained as the optimal lining thickness in the domain of the test, with a modest improvement in the performance of the lining, the main economic basis being the increase in operational durability of the lining (Table 3).

The solar still, composed of glass, water, and a basin liner, attains a higher temperature using an 8 mm cotton cloth lining rather than the standard 4 mm, as depicted in Figure 5. This difference could result from the thicker cotton fabric of the solar still, which enhances water absorption through capillarity from the basin. Consequently, the temperatures of the water, glass, and basin liner increase, while the water capacity of the basin decreases. Figure 6 illustrates the impact on fresh water production in a modified single-slope solar still.

As observed in Figure 7, the vapour temperature within the cotton fabric stills remains notably lower compared to that in traditional solar stills. This discrepancy in temperature could be attributed to the presence of water in the 8 mm cotton cloth lining still, which can absorb the heat energy emanating from the vapour side.

As seen in Table 4, the water quality analysis showed that there was a considerable decrease in the total dissolved solids (TDS), electrical conductivity (EC) and turbidity after desalination. The water parameters obtained from the distillate of the water samples meet the WHO drinking water standards, which show that the proposed solar still system produced freshwater effectively. At optimum operating conditions, water quality parameters were measured for the feed saline water, and the distillate water collected from the modified solar still with the thickest wall lining (8 mm). The feed water had a TDS of 3500 ± 50 ppm, pH of 7.8 ± 0.1, electrical conductivity (EC) of $5800 \pm 80\,\mu$S/cm, and turbidity of 3.2 ± 0.4 NTU. The collected distillate exhibited a TDS of 12 ± 3 ppm, pH of 6.9 ± 0.1, EC of $22 \pm 5\,\mu$S/cm, and turbidity below 0.5 NTU. The World Health Organisation (WHO, 2017) drinking water quality guidelines are followed for all distillate quality parameters (TDS $\leq$ 500 ppm, pH 6.5–8.5), showing that the solar still is performing well in the removal of dissolved salts and thus producing potable freshwater. The efficiency of the TDS removal of the solar still is $(3500\text{–}12)/3500 \times 100 = 99.66\%$, which is similar to the efficiency reported by the passive solar still in similar studies.

The productivity of the solar stills at a daily and hourly rate can be observed in Figure 8. The total freshwater productivity of the 8 mm configuration was 2.330 L (4.66 L/m^2/day). The corresponding values for wall thicknesses of 0 mm, 4 mm and 8 mm were 1.26, 2.23, and 2.330 L, with 1260 mL/day, 2230 mL/day, and 2330 mL/day (2.52, 4.46, and 4.66 L/m^2/day), respectively. The output mentioned is for a 0.5 m^2 area per day (24 hours). Freshwater productivity increased with the increase in effective evaporation area. Figure 9 shows a noticeable variation in freshwater output between the 4 mm and 8 mm wall lining thickness configurations across all test intervals, with both setups exhibiting higher productivity compared with the other configurations. There is no difference in the 4 mm and 8 mm wall lining design, other than the number of layers of cotton cloth that are applied to the inner walls of the basin. The observed improved freshwater productivity for the 8 mm configuration was achieved due to the combined effects of increased evaporative surface area with enhanced capillary water uptake, and of reduced conductive heat loss through the basin walls and of maintaining a slightly higher basin water temperature. This outcome is certainly connected to the exceptional performance of the 8 mm, which is

Table 3. Experimental results of single slope solar still.

	Conventional still				4 mm thick wall				8 mm thick wall			
Time	Basin Temp (T_b) (^0C)	Glass Temp (Tg) (^0C)	Water Temp (Tw) (^0C)	Vapour Temp (Tv) (^0C)	Basin Temp (T_b) (^0C)	Glass Temp (Tg) (^0C)	Water Temp (Tw) (^0C)	Vapour Temp (Tv) (^0C)	Basin Temp (T_b) (^0C)	Glass Temp (Tg) (^0C)	Water Temp (Tw) (^0C)	Vapour Temp (Tv) (^0C)
9	44.5	44.75	41	43.5	47	43.75	43.5	44	43	45.5	43.75	45.5
10	48.5	50	51	55	54.5	51.25	51.5	51.5	52.5	51.25	53.5	54.5
11	59	54.25	58.5	64	62.5	58.75	59	58.5	60	59	60.5	60.5
12	68	54.75	61	66	68	62.75	65.5	62	62.5	63.5	64.5	62
1	68	53.25	59.5	66.5	68.5	61.75	68	63	61.5	63.25	63.5	60
2	65.5	51.25	56.5	64.5	66.5	59.5	67	63	59	60.75	61.75	56.5
3	61	46.75	51	60	63.5	57.5	65.5	61	52.5	58	59	51
4	55	42.25	47	53.5	61.5	54.25	63.5	59.5	51	54.25	56.25	47

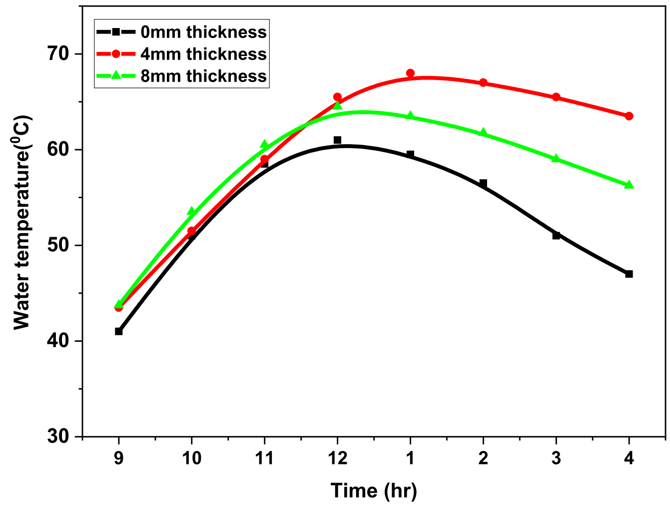

Figure 5. Comparison of water temperatures in conventional and modified solar stills.

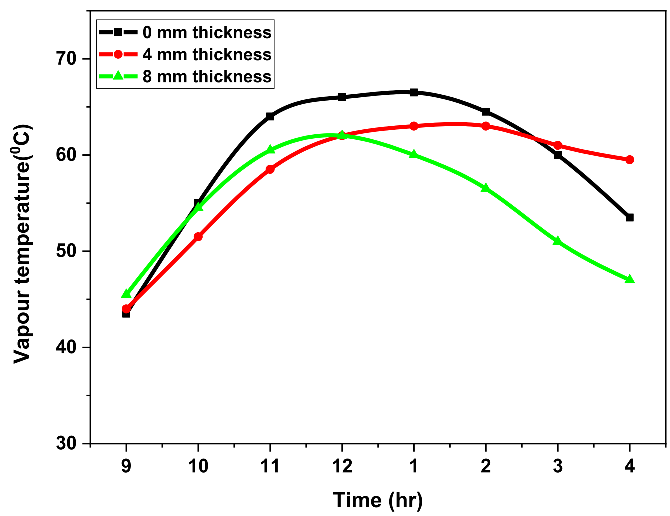

Figure 6. Comparison of vapour temperatures in conventional and modified solar stills.

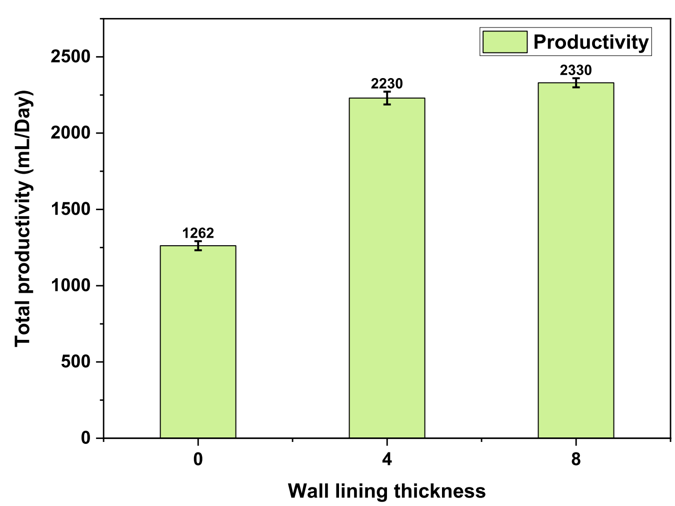

Figure 7. Total productivity of single slope solar still with varying wall lining thicknesses.

Table 4. Water quality analysis of feed water and distilled water obtained from the single-slope solar still system.

Parameter	Feed water (input)	Distillate (output)
Total dissolved solids – TDS (ppm)	3500 ± 50	12 ± 3
pH	7.8 ± 0.1	6.9 ± 0.1
Electrical conductivity – EC (µS/cm)	5800 ± 80	22 ± 5
Turbidity (NTU)	3.2 ± 0.4	< 0.5
WHO drinking water guideline (TDS, ppm)	–	≤ 500
WHO drinking water guideline (pH)	–	6.5–8.5

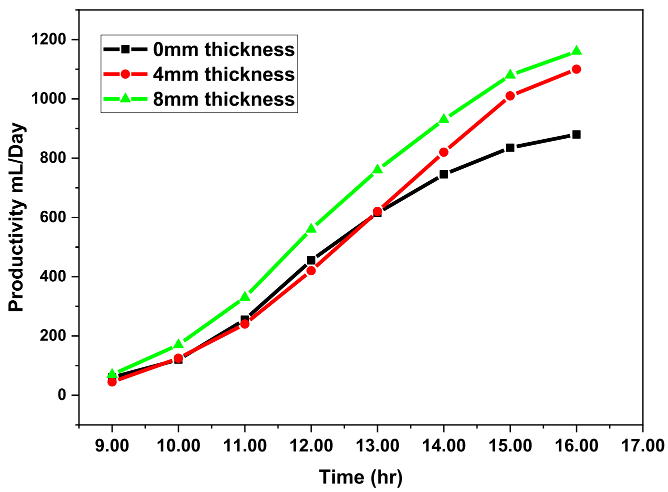

Figure 8. Daily productivity of conventional and modified single slope solar stills with varying wall lining thicknesses.

achieved through its ability to operate within the highest temperature ranges. The enhanced productivity was observed for modified solar still is 27.7% and 31.6% for the 4 mm and 8 mm configurations, respectively.

Figure 9 illustrates the meteorological conditions observed during cover cooling at varying flow rates. The irradiation data for four particular days selected during the experiment are presented in Figure 9 (a). This figure indicates minimal variation in solar radiation intensity, attributed to consistent weather patterns throughout the observed period. Ranging from its minimum at daybreak to its peak at noon, the solar irradiance fluctuated, reaching a maximum value of 950 W/m^2. Analysis of the air temperature data for four different days, as shown in Figure 9 (b), reveals a consistent similarity in the recorded air temperatures, with minimal discernible differences between them. Furthermore, the illustration in Figure 9 (c) displays the varying wind speeds on different days for cooling water. It can be observed that the variation between the days is minimal, with wind speed fluctuating between 1.2 and 4 m/s.

5.2. Response surface methodology

The statistical software was used as a simple statistical tool to design experiments to determine the experimental conditions. To achieve the desired operating conditions, a Central Composite Design (CCD) was utilised in this study. The Response Surface Methodology (RSM) showcased the optimal conditions for maximising distilled water production. This was accomplished by extensively examining the impact of critical factors such as wind speed, wall thickness, solar radiation, and ambient temperature. The enhancing design parameter for fresh water productivity of coded value is shown in Table 5.

The selection of parameters for optimisation in our investigation is grounded on their notable influence on the productivity and efficiency of solar distillation systems, as supported by prior research and empirical findings. Specifically, the parameters selected – ambient temperature, wall thickness, solar radiation, wind velocity, and wall lining thickness (cotton cloth) are critical because they directly influence the thermal dynamics and evaporation-condensation processes within the solar still. Ambient temperature and solar radiation are primary drivers of the thermal energy available for water evaporation. Wall thickness and wall lining thickness affect heat retention and loss, which are crucial for maintaining optimal internal temperatures. Wind velocity affects the cooling rate and condensation efficiency, thereby influencing the overall productivity of the solar still. By focusing on these parameters, our optimisation analysis aims to enhance the understanding of their interrelationships and cumulative effects, leading to improved design and operational strategies for solar stills. The output responses for various parameter interactions are shown in Table 6. This comprehensive approach ensures that the most influential factors are accounted for, thereby maximising the efficiency and yield of the system.

5.2.1. Analysis of variance (ANOVA)

Analysis of Variance (ANOVA) evaluates the accuracy of a model, as indicated in Table 7. This study's components are the sum of squares, degrees of freedom (DOF), *P*-values, F-values, and adjusted mean squares. The F-value measures the data's variance from the mean. The F-test result of 144.53, coupled with a *p*-value below 0.0001, signifies the proposed model's importance. The *p*-value serves as an indicator for determining the threshold of importance required to reject the null hypothesis. Additionally, the *P*-values serve as a benchmark for assessing the model's validity from a statistical perspective. The freshwater productivity prediction of the quadratic model developed by the least squares method, as expressed in terms of polynomial Equation expressed as

$$\begin{aligned}\text{Daily Productivity} = {} & +1238.657 - 8.111 * A \\ & + 50.9444 * B + 673.5 * C \\ & + 10.555 * D + 15.4375 * AB \\ & - 9.8124 * AC - 7.6874 * AD \\ & + 70.4375 * BC + 14.5625 * BD \\ & - 3.9374 * CD + 57.6842 * A^2 \\ & + 30.1842 * B^2 + 123.1842 * C^2 \\ & + 29.6842 * D^2\end{aligned}$$

The daily productivity of the coded equation, expressed through encoded factors, is used to predict potential outcomes based on the predefined levels of each factor. By default, the elevated levels of the factors are encoded as positive ones, whereas the reduced levels are encoded as negative ones. The encoded equation is advantageous for discerning the comparative influence of the factors by contrasting the coefficients of the factors.

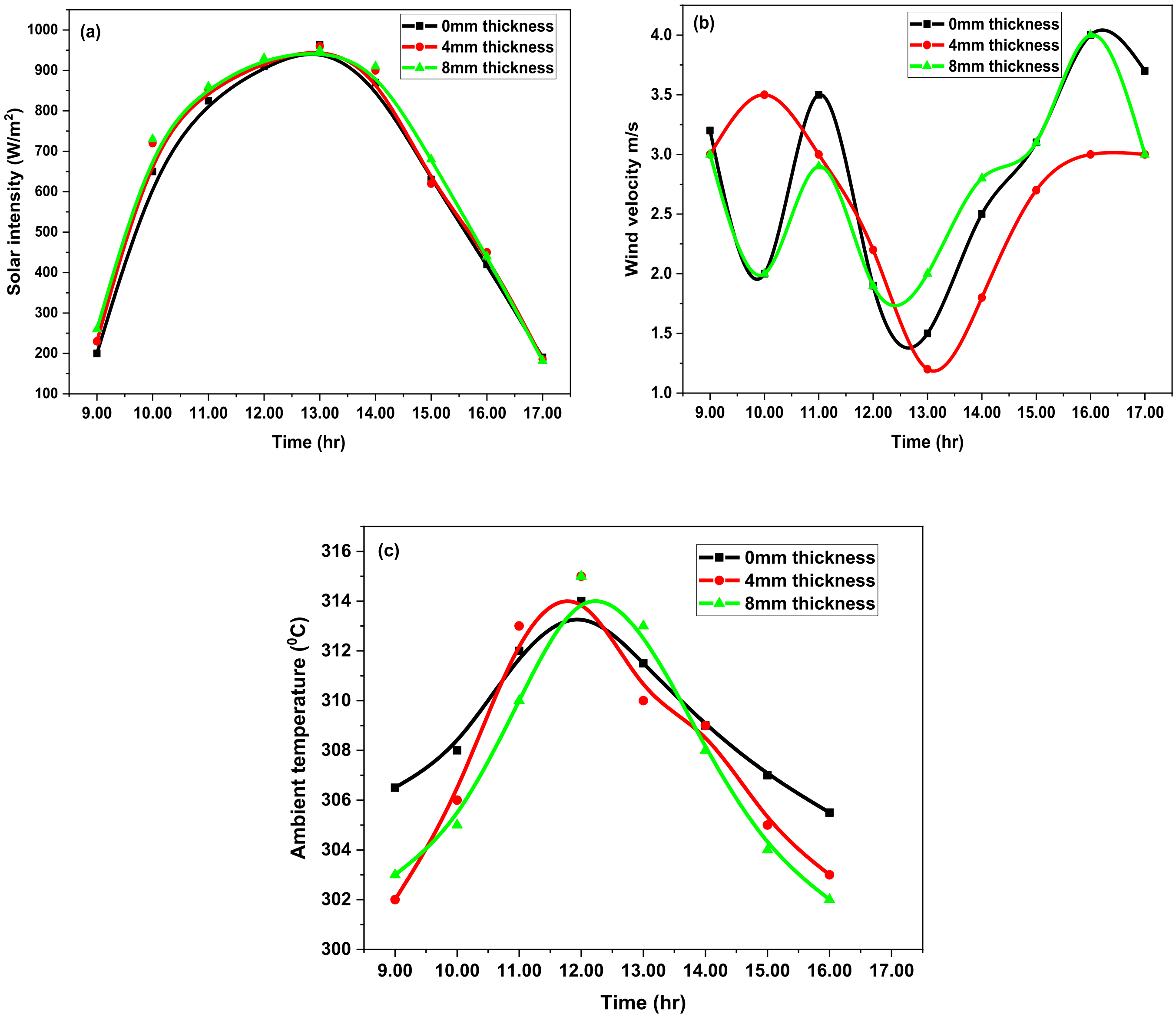

Figure 9. Environmental conditions during the experiment (a) solar intensity, (b) wind speed, (c) ambient temperature.

Table 5. Design parameter for fresh water productivity.

		Levels		
		−1	0	1
Variables	Units	Minimum	Average	Maximum
Ambient temperature	°C	30	35	40
Wall thickness	mm	0	4	8
Solar radiation	W/m^2	300	600	900
Wind velocity	m/s	1	1.5	2

The null hypothesis for the ANOVA indicates that the Lack of Fit (F = 83.50 and $p < 0.0001$) is statistically significant, but this is not conflicting with the high R^2 value of 0.9926. The F value for the Lack of Fit is the ratio of the variance at the non-centre point runs (MS Lack of Fit = 6371.19) to the pure error variance estimated at the six replicated centre point runs (MS Pure Error = 76.30). The pure error denominator is very small (SD = 9.4 mL/day, CV = 0.75%), which gives a very large Lack of Fit F-value, even though the absolute sum of squares (63,711.90) accounts for less than 0.74% of the total sum of squares (8,710,000). As the high Predicted R^2 (0.9595) and Adequate Precision (34.98) confirm, the model is still very good for prediction and optimisation. The residual plot in Figure 10, illustrates the relationship that must be utilised in conjunction with the fitted data to evaluate the accuracy of the RSM model. In these graphs, each response variable is examined independently. Figure 10 (a–b), which presents the normal probability plot of the residuals, is used to verify the normality of the data. These plots exhibit a linear trend. The linearity of the residual distribution suggests a normal distribution, signifying a good fit between the regression model and the observed data (Haitham, Jamel, and Ihab 2020). The diagrams also show a positive correlation between the fitted and observed values, confirming the suitability and relevance of the RSM model (Yuvaperiyasamy et al. 2025).

Furthermore, Table 6 contains the R-squared (R^2) and adjusted R-squared (R^2-adj) values, which serve to demonstrate the exceptional precision of the utilised model. These values

Table 6. Effect of single solar still parameter contribution on fresh water productivity.

		Factors				Response 1
Std	Run	A: Ambient temperature	B: Wall thickness	C: Solar radiation	D: Wind velocity	Daily productivity
Units		C	mm	W/m^2	m/s	mL/day
11	1	35	4	600	1	1250
6	2	30	8	300	1	750
9	3	35	4	900	1.5	1900
4	4	35	4	600	1.5	1250
30	5	40	4	600	1.5	1300
8	6	30	0	300	2	775
29	7	40	8	300	2	770
5	8	35	4	600	1.5	1245
12	9	40	8	300	1	760
3	10	30	0	900	2	2110
10	11	30	8	900	2	2320
15	12	40	0	300	1	790
26	13	35	4	300	0	800
28	14	40	8	900	2	2330
21	15	35	4	600	1.5	1260
27	16	35	4	600	1.5	1240
19	17	35	4	600	1.5	1263
1	18	30	0	900	1	2105
17	19	35	8	600	1.5	1252
18	20	40	8	900	1	2315
14	21	30	8	300	2	840
7	22	35	0	600	1.5	1262
24	23	40	0	900	2	1950
25	24	40	0	900	1	2003
23	25	35	4	600	2	1263
22	26	30	8	900	1	2230
20	27	40	0	300	2	845
2	28	30	4	600	1.5	1269
16	29	35	4	600	1.5	1251
13	30	30	0	300	1	810

Table 7. Analysis of variance (ANOVA).

Source	Sum of squares	df	Mean square	*F*-value	*p*-value	
Model	8.646E + 06	14	6.176E + 05	144.53	< 0.0001	Significant
A-Ambient Temperature	1184.22	1	1184.22	0.2771	0.6063	
B-Wall thickness	46716.06	1	46716.06	10.93	0.0048	
C-Solar Radiation	8.165E + 06	1	8.165E + 06	1910.85	< 0.0001	
D-Wind Velocity	2005.56	1	2005.56	0.4694	0.5037	
AB	3813.06	1	3813.06	0.8924	0.3598	
AC	1540.56	1	1540.56	0.3605	0.5572	
AD	945.56	1	945.56	0.2213	0.6448	
BC	79383.06	1	79383.06	18.58	0.0006	
BD	3393.06	1	3393.06	0.7941	0.3869	
CD	248.06	1	248.06	0.0581	0.8129	
A^2	8621.17	1	8621.17	2.02	0.1759	
B^2	2360.54	1	2360.54	0.5524	0.4688	
C^2	39315.36	1	39315.36	9.20	0.0084	
D^2	2282.99	1	2282.99	0.5343	0.4761	
Residual	64093.40	15	4272.89			
Lack of fit	63711.90	10	6371.19	83.50	< 0.0001	Significant
Pure error	381.50	5	76.30			
Cor total	8.710E + 06	29				

R^2-0.9926, Adjusted R^2-0.9857, Predicted R^2-0.9595, Adeq Precision-34.98.

were closely approximate to unity for freshwater productivity. This finding implies a robust empirical correlation between the dependent and independent variables. Consequently, the commendable performance of the RSM model can be attributed to the fact that the F-values for the response exceed unity. Additionally, the statistical validation of the model is evident, as indicated by the *P*-value being less than < 0.0001. The *p*-value is expressed as the decision point for excluding values to determine the minimal significance level required to reject the null hypothesis.

Table 8 presents the validation analysis of the single-slope solar still by comparing the experimentally obtained freshwater productivity with the predicted output values under optimised operating conditions. The close agreement between the experimental and predicted results confirms the accuracy and reliability of the developed regression model. Three measures were used to determine the degree of overfitting. The R^2 is 0.9926 and the Predicted R^2 (computed with the leave out one cross validation statistic) is 0.9595, with a difference of only 0.0331 within the accepted limit of 0.2, indicating good generalisation

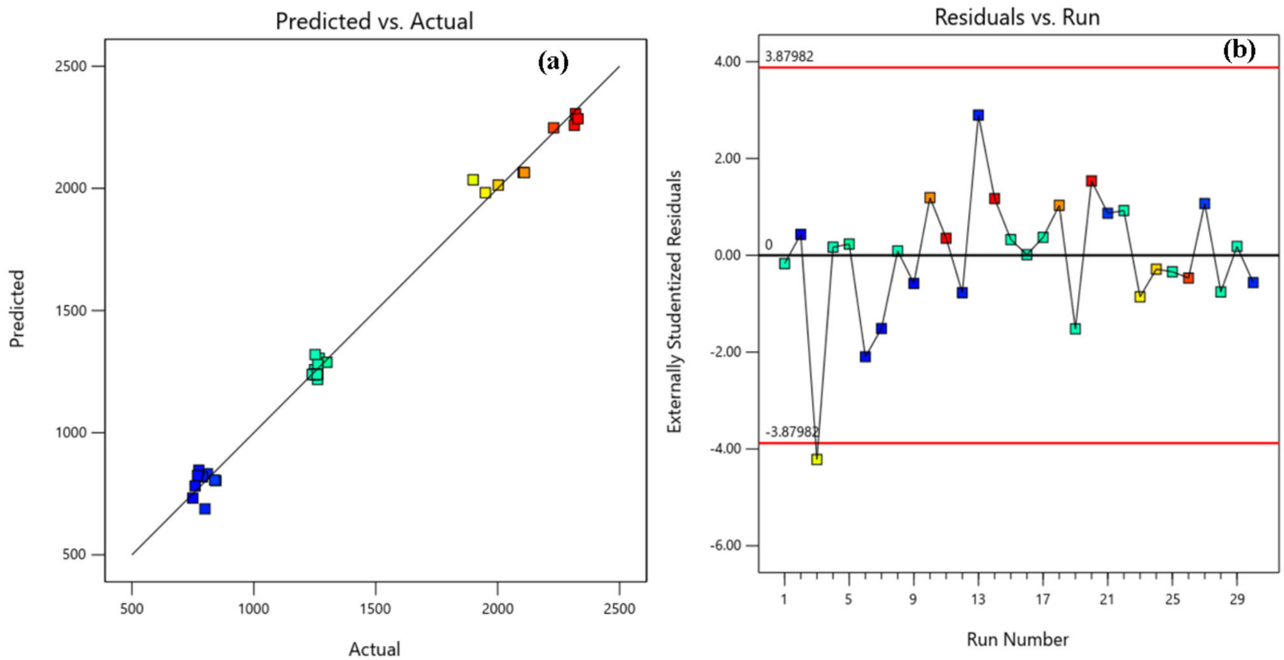

Figure 10. Residuals generated by Response Surface Methodology (RSM) with the daily productivity of a solar still (a) predicted values, (b) externally studentised residuals.

Table 8. Validation analysis of single -slope solar still for obtained output.

Validation metric	Value obtained	Threshold / criterion	Status
R^2	0.9926	–	Excellent model fit
Adjusted R^2	0.9857	Should be close to R^2	Difference = 0.0069 (Accepted range)
Predicted R^2 (PRESS)	0.9595	R^2 − Pred.R^2 < 0.20	Difference = 0.0331 (Accepted range)
Adeq precision	34.98	> 4.0 required	9× above threshold (Accepted range)
Experimental validation error	1.96%	< 5% acceptable	Within limits (Accepted range)
Centre-point repeatability (SD)	±9.4 mL/day	Low SD indicates precision	Confirms reproducibility (Accepted range)

ability of the model. All 14 model terms are meaningful contributors as shown by the Adjusted R^2 of 0.9857. The Adequate Precision ratio (signal-to-noise ratio) is 34.98 (threshold > 4.0). Furthermore, an independent experimental validation test was performed at the RSM optimised conditions and the results were 2330 mL/day, which corresponds to only 1.96% error when compared to the model prediction of 2285 mL/day, demonstrating the model's predictive accuracy on unseen data. The results as a whole show that the quadratic model is not overfitting the data.

5.2.2. Main effect plots on productivity

The plots shown in Figure 11 (perturbation plots) show the sensitivity of daily freshwater productivity to each of the four optimisation variables when the other variables are kept at their centre values. Similar to the ANOVA results (Table 6), the response gradient of solar radiation (C) is highest of the four factors (1400 mL/day) and productivity increased from 800 mL/day at 300 W/m^2 to 2200 mL/day at 900 W/m^2, confirming its dominant role (F = 1910.85, p < 0.0001). The thickness of the wall lining (B) has a moderate positive slope, with productivity rising by about 150 mL/day when the thickness of wall lining increases from 0 mm to 8 mm, under the centre-point conditions (F = 10.93; p = 0.005). The interaction between wall lining thickness and solar radiation (BC) is also statistically significant (F = 18.58, p = 0.0006) meaning that the highest solar radiation the greater the benefit of wall lining. The linear responses of

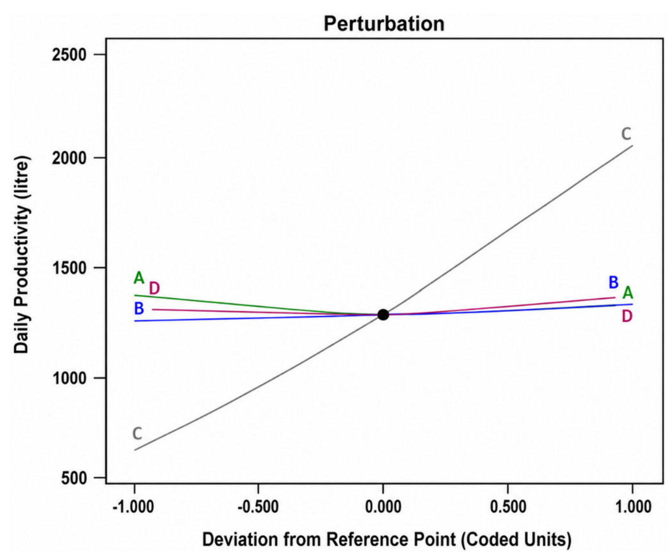

Figure 11. Perturbation plots for daily productivity using single slope solar still.

ambient temperature (A) and wind velocity (D) to the perturbations are almost flat and the ANOVA results indicate that these factors are not significant (F = 0.28, p = 0.606 and F = 0.47, p = 0.503 respectively). The apparent convergence of all four curves in the centre point is a plotting feature due to the common value of productivity of the centre point (1250 mL/day),

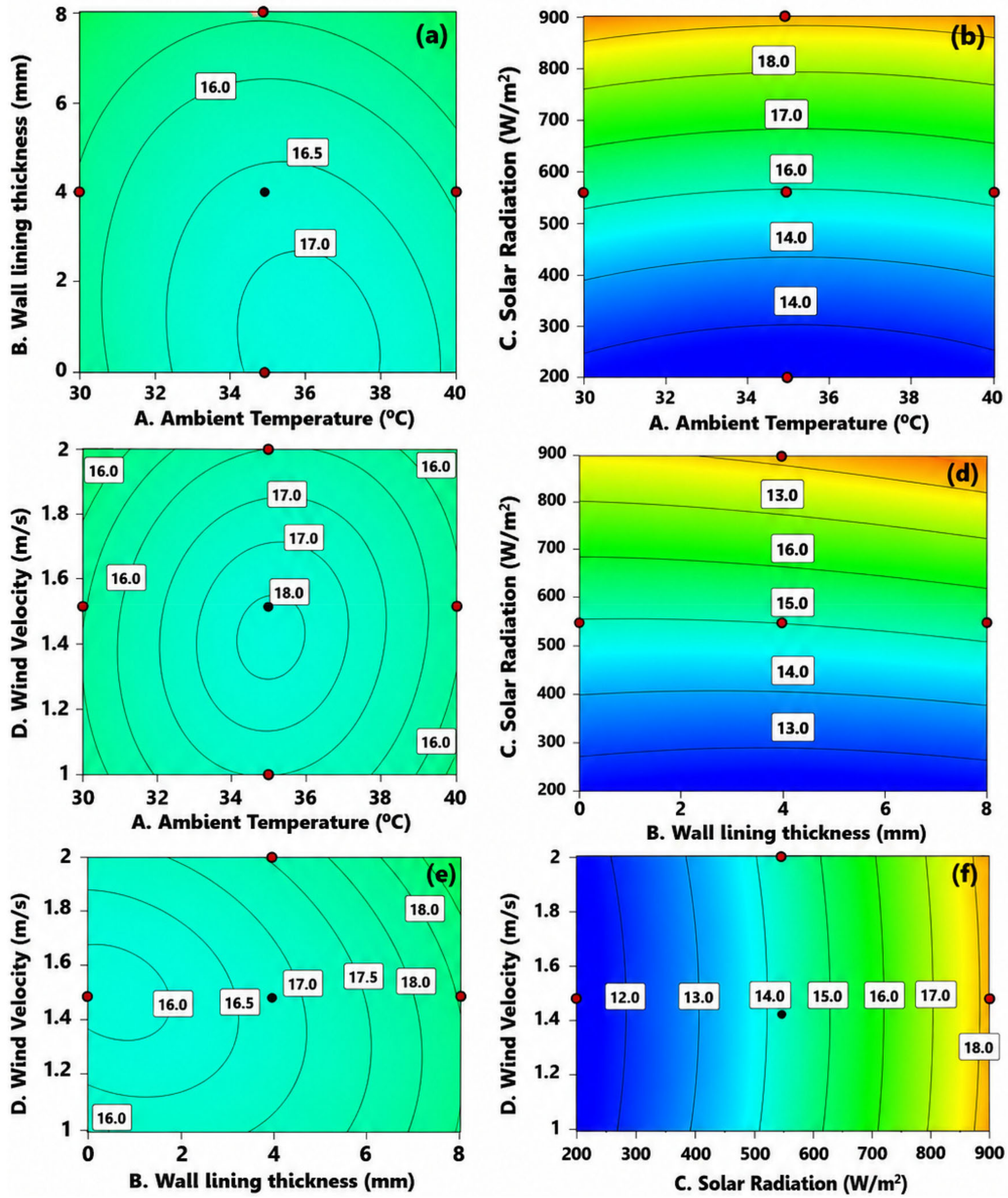

Figure 12. 2D Response surface plot of interaction between parameters on freshwater productivity (a) A.B. (b) A.C. (c) A.D. (d) B.C. (e) B.D. (f) CD (Note: A: Ambient Temperature, B: Wall thickness, C: Solar Radiation, D: Wind Velocity).

but the distinct divergence of the solar radiation curve from the centre point clearly demonstrates the superiority of the solar radiation curve.

5.2.3. Effect of solar still parameters on freshwater productivity

Freshwater productivity is shown in these 2D (Figure 12 a–f) and 3D (Figure 13 a–f) response surface plots as affected by the four optimisation parameters. The increases in productivity are driven by four different physical mechanisms with different subsets of the optimisation variables that are discussed below. Freshwater productivity is primarily driven by solar radiation, which directly provides the thermal energy needed to evaporate water from the surface of the basin. The higher the solar irradiance, the more heat is absorbed and the higher the temperature of the water in the basin (Tw). The evaporation rate is controlled by the difference in vapour pressure between the hot water surface and the cooler inner surface of the glass cover; higher vapour pressure differential implies that more water vapour will flow to the inner surface of the glass cover. The ANOVA result for solar radiation (Factor C, $F = 1910.85, p < 0.0001$) confirms this physical relationship as it is by far the most statistically significant parameter in this study. From Figures 12 and 13(b), it is observed that by increasing the solar radiation from 300 W/m^2 to 900 W/m^2 (for 40°C ambient temperature and 8 mm wall lining thickness), the daily productivity increases from about 770 mL/day to

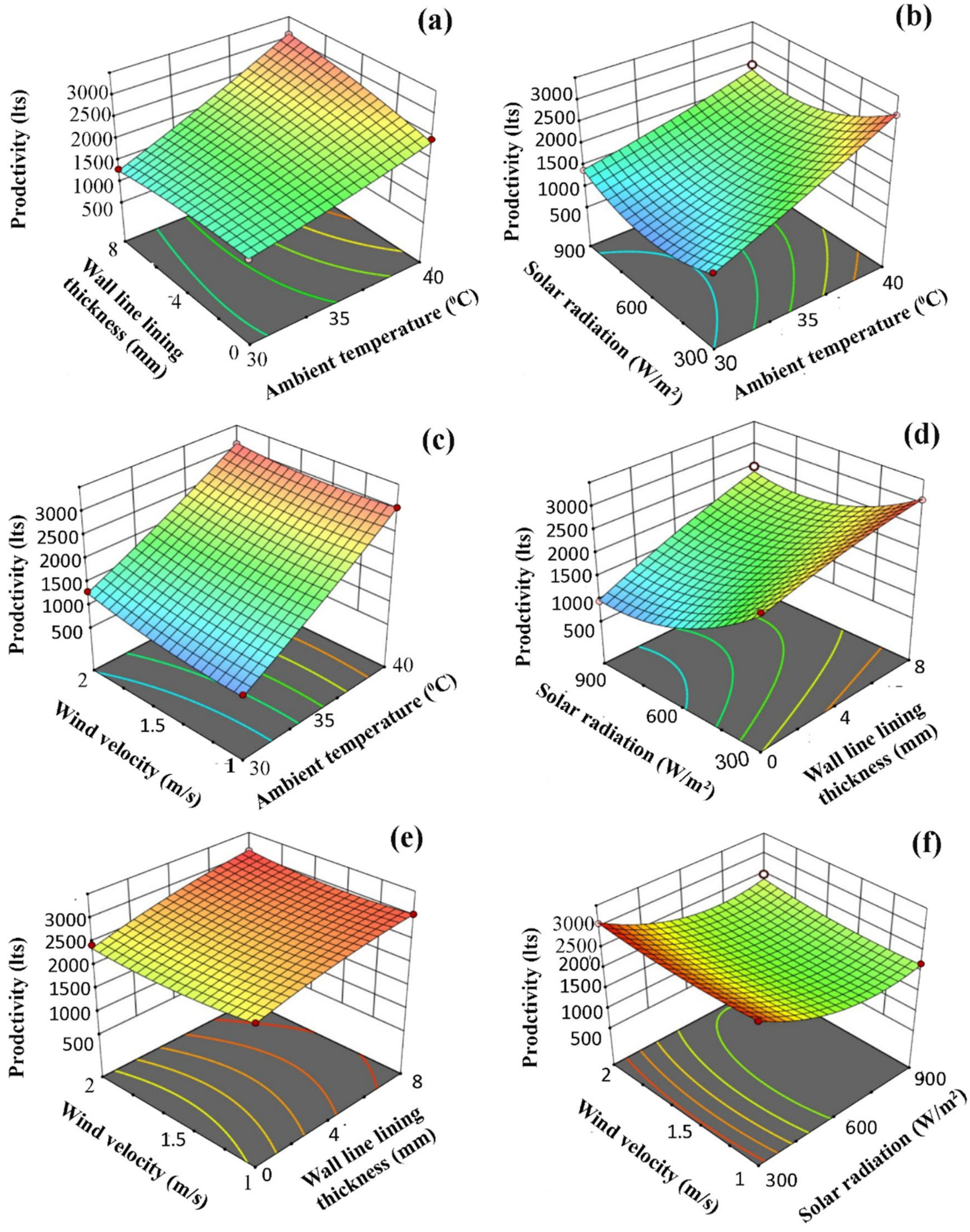

Figure 13. 3D Response surface plot of interaction between the parameters on fresh water productivity (a) A.B. (b) A.C. (c) A.D. (d) B.C. (e) B.D. (f) CD. (Note: A: Ambient Temperature, B: Wall thickness, C: Solar Radiation, D: Wind Velocity).

2330 mL/day. The cotton cloth wall lining also helps to enhance evaporation by capillary action – water moves up through the cotton cloth above the static water level, which increases the wetted evaporative surface area. The large 4 mm lining saw a near total improvement in wetting of the inner basin wall, which is responsible for the large productivity gain (+77%). The extra layer in the 8 mm configuration brings a relatively small, but still positive, advantage (+4.5%) from 4 mm to 8 mm due to the increased wetted area.

Heat retention is the ability of the solar still to keep a high-water temperature in the basin during the test day, which helps to reduce heat loss from the sides, base and glass cover of the solar still. The cotton cloth wall lining (0–8 mm) is placed between the hot saline water and the wooden wall to provide a layer of material with low thermal conductivity to the side walls of the basin and thus reduce the conductive heat loss. This reduction in the evaporator loss through the wall helps to maintain a higher Tw for longer, delaying the onset of evaporator operation to late afternoon when the solar irradiance decreases. The temperature profiles in Figure 3 also show that the 8 mm lining configuration keeps higher T_w values than the other two configurations: 4 mm and conventional (0 mm) for all hours of the test day, especially after 14:00. The thermocol insulation layer (25.4 mm) below the basin also helps to minimise conductive heat transfer in the downward direction. All of these insulating elements combine to cause the absorbed solar energy to be used for latent heat of evaporation instead of being lost as sensible heat to the ambient.

The last productive step in the solar still cycle is condensation of water vapour on the surface of the glass cover. The rate of condensation is controlled by the difference in temperatures between the water vapour (T_v) and the inner surface of the glass cover (T_g): a bigger difference in temperature ($T_v - T_g$) between the two leads to faster condensation of water vapour and higher distillate production rate per unit time. This differential is maintained by two processes: (i) the solar radiation and wall heat retention discussed above keep Tw and, consequently, Tv at a high value; and (ii) the conductive-convective heat transfer from the outer surface of the glass keeps T_g lower than T_v. The experimental data in Figures 4–6 show that T_g is always lower than both Tw and T_v during the test day, which allows for continuous condensation to proceed, as desired. The greater the (Tw − Tg) differential, the greater the amount of distillate that is recovered, and the 8 mm lining configuration exhibits the highest ($T_w - T_g$) differentials of the three configurations, thereby resulting in the highest distillate product yield. Ambient temperature (40°C) also affects the system by raising T_w above T_g, which increases the condensation driving temperature difference in the still.

There are two competing mechanisms that occur simultaneously in the solar still and should be considered together to properly interpret the productivity trends in this study: wind velocity, and wind power density. The convective heat transfer coefficient at the outer glass surface (h_{ext}) increases, due to the external wind flow over the inclined glass cover, which enhances the heat transfer from the outer glass surface to the ambient air. This reduces the surface temperature of the outer glass surface (T_g), thus creating greater difference in temperature between the vapour and the glass surface ($T_v - T_g$) that will accelerate condensation of water vapour onto the inside of the glass. This positive impact is the most pronounced in the range of wind speeds of 1-2 m/s tested. The detrimental effect also increases the convective heat transfer rate from the outside surface of the glass to the ambient air for the same increase in h_{ext}. This heat loss is ultimately extracted from the thermal energy stored in the basin water, which over time will tend to reduce T_w. At very high wind speeds, the negative heat loss mechanism can outweigh the positive condensation enhancement and cause a negative overall impact on the water temperatures, evaporation rates and productivity of the basin.

In the tested range (1–2 m/s) of wind velocity, the condensation-enhancement effect dominates, as evidenced by the positive coefficient of the wind velocity (D, +10.555) in the regression model and the positive trend in productivity shown in Figures 12(c) and 13(e). The ANOVA result for wind velocity ($F = 0.47$, $p = 0.503$) shows a positive but small net value with the two opposite effects almost balanced, with the condensation enhancement slightly weighting the net value. This is in line with the results presented by Keshtkar et al. (2020), which show that productivity gains increased by 14.4% as wind speed increased from 1 to 6 m/s, which is far more than the beneficial wind speed of 2 m/s. This research should be extended to include wind speeds greater than 2 m/s to determine the threshold wind speed at which there is a crossover in the heat loss penalty becoming more significant, which can be used to guide site selection for applications in high wind conditions.

5.3. Optimisation

The parameter combination which yielded the maximum freshwater productivity within the experimental domain tested was identified from the RSM-CCD desirability function, and the optimum results obtained are shown in Table 9. The maximum ambient temperature tested is 40°C, which is the maximum possible ambient temperature in the test region (Chennai, India, from March–May). The lower the difference between the water temperature in the basin and the surrounding air temperature, the less heat will be lost from the outside through the basin walls, resulting in better thermal retention and higher water temperature in the basin. The maximum thickness tested for a wall lining was 8 mm. This thickness of 8 mm cotton cloth lining achieves a lesser conductive heat loss from the back wall and side walls while maintaining a greater wetted evaporative surface area due to capillary action. The productivity gain between 4 mm and 8 mm was slightly less than 4.5%, compared to 77% between 0 mm and 4 mm, suggesting a decreasing return to thickness. The upper limit of 8 mm was set by practical considerations: increasing the thickness of the lining gradually decreases the amount of water inside the basin, and changes the capillary wicking effects of the cotton cloth. It is also remarked that the productivity gain of the system between 4 mm and 8 mm wall lining thickness is only 4.5%, suggesting that within the thickness range tested, the system is moving towards a performance plateau at 8 mm. Wall lining thicknesses greater than 8 mm, up to approximately 16 mm, warrant further investigation to determine the actual performance limit and to establish whether an increased thermal mass penalty is introduced with increasing thickness, which could eventually reverse the observed trend of enhanced productivity. Further investigation is recommended for wall lining thicknesses in the range of 8 mm to 16 mm to determine whether 8 mm represents the optimum point in the productivity–thickness relationship. The maximum solar radiation recorded at the test site during the summer experimental period was considered the upper limit of the tested range, corresponding to 900 W/m^2.

Solar radiation is the most dominant parameter (ANOVA F value 1910.85, $p < 0.0001$) that directly contributes to the increase in water temperature of the basin and hence to the evaporation speeds that lead to better condensation of the water vapour and distillate production. The maximum temperature difference between water surface and the glass cover in the basin was observed at the highest speed of wind, which was 2 m/s in the tested range. This condition enabled continuous condensation and efficient collection of condensate droplets from the inner glass surface, thereby maximising distillate yield. The condensation-enhancement effect of wind outweighed the other external heat loss mechanism in the range of wind speeds tested (1–2 m/s). The RSM model had a prediction error of 1.96%

Table 9. Optimised parameters for single-slope solar still.

Output responses	Objective	Ambient temperature	Wall thickness	Solar radiation	Wind velocity	Expected optimum response	Experimental	Error
Productivity	Maximise	40	8	900	2	2285 mL/day (4.57 L/m^2/day)	2330 ml (4.66 L/m^2/day)	1.96%

Table 10. Comparative analysis between the present optimised single-slope solar still and advanced configurations.

Design type	Productivity (L/m^2/day)	Thermal efficiency (%)	Cost indicator (Rs. /m^2)	Fabrication complexity	Maintenance
Conventional single-slope (0 mm lining, this study)	2.52	22%	12,000	Very Low	Very Low
Optimised single-slope (8 mm lining, this study)	4.66	31.6%	18,680	Very Low	Low
Stepped solar still [28]	4.8–5.5	35–40%	25,000–35,000	Medium	Medium
Pyramid solar still (Senthilkumar, Yuvaperiyasamy, and Deepanraj 2024)	3.5–4.5	28–35%	22,000–30,000	Medium	Low–Medium
Double-slope solar still (Garg 1975)	3.0–4.0	25–32%	20,000–28,000	Low–Medium	Low
Water-jacket solar still (Srivastava and Agrawal 2013)	5.2 (4.46 L/m^2/day)	43.19% higher vs. CPSS	30,000+	Medium	Medium
Multi-effect solar still (Srivastava and Agrawal 2013)	6.0–10.0	50–70%	80,000–150,000	High	High

for the freshwater productivity, and was validated with the experimental value of 2330 mL/day (4.66 L/m^2/day for the 0.5 m^2 basin), which shows a good accuracy of the quadratic regression model under the given boundary conditions.

It is crucial to note that all three of the controlled optimum values (40°C, 8 mm, 900 W/m^2) correspond to the maximum values of the experimental domain. This suggests the response surface still rises in these directions and that the actual mathematical optimum might be outside the test range, which is a known disadvantage of bounded RSM-CCD optimisation. The practical upper limits selected in this study were determined partly by the seasonal climatic ceiling of the test site, as solar radiation and ambient temperature cannot exceed their natural maximum values, and partly by the constraints imposed by the basin geometry and wall lining thickness. Further studies are recommended to extend the operating boundaries by employing reflector panels to increase solar radiation up to 1100 W/m^2 and by increasing the wall lining thickness to 16 mm to determine whether a maximum performance limit can be achieved using low-cost reflector panels.

The present results are limited to the experimental domain (30–40C, 300–900 W/m^2 solar radiation, and 1–2 m/s wind velocity) and the specific climatic condition of Chennai, India during the summer season. This model should not be extrapolated outside the range or used directly in various climate zones without re-validating the model. In addition, absolute productivity values in published solar still studies cannot be directly compared with other studies, as basin area, water salinity and initial water depth were different in different studies, and only relative changes and improvements in the solar still are compared in this study. Qualitatively, the model predicts continued positive productivity gains with increasing solar radiation (linear coefficient +673.5) and wall lining thickness (linear coefficient +50.9) within the linear regime. Application to other climatic zones (humid coastal, semi-arid, temperate) would require re-calibration of the model with new experimental runs at the relevant boundary conditions, and the addition of relative humidity as a variable where vapour pressure deficit is a significant constraint.

The results of comparison between the present optimised single-slope solar still and previously reported advanced solar still configuration are presented in Table 10. The comparison shows that, under realistic operating conditions, the proposed system has competitive freshwater productivity with economic feasibility. The optimised single-slope solar still (with a lining of 8 mm cotton cloth and solar still productivity of 4.66 L/m^2/day, thermal efficiency of 31.6%) has productivity comparable to that of stepped and pyramid solar still designs at a capital cost of about 40–50% lower. Multi-effect stills and water-jacket configurations have higher peak efficiencies, but require 2 to 8 times more initial investment and more complicated maintenance, making them less useful for the most applicable situation of the off-grid, resource-limited environment for which the single-slope design is best suited. The major benefit is that it increases productivity by 85% as compared to the conventional single-slope design by the simple and low-cost material modification—cotton cloth lining— $<$ Rs. Without adding extra mechanical complexity or maintenance issues, 1,000 incremental costs.

5.4. Cost analysis

The expenses incurred in creating a single liter of pure water from the existing solar distillation systems over their operational lifetime are detailed in Table 11. The market value of a litre of clean drinking water stands at Rs.19.88. The cost component breakdown provides insight into the financial considerations of implementing a single-slope solar still. It covers various aspects such as materials, fabrication, installation, and operational costs. The total initial cost amounts to Rs. 9,340.00, including all materials, labour, and initial maintenance expenses. Annual maintenance costs are estimated at Rs. 500.00, contributing to the total annual cost. Finally, the cost per litre of distilled water produced, calculated as the initial cost spread over the first year, is approximately Rs. 19.88. The expanded techno-economic analysis shows: (i) cost per litre of Rs. 10 per litre for 10 years on average, (ii) an average payback period of 10 years. As per base-case condition (300 effective operating days/year, 1650 mL/day average output), (iii) simple payback period of 2.5–4 years as compared to retail packaged water at Rs. 10 to 20/L; (iv) net saving of around Rs. 59,910 over 10 years for one unit of 0.5 m^2 and (v) economic viability confirmed even under the pessimistic

Table 11. Cost analysis for single-slope solar still.

Cost component	Description	Unit cost (Rs)	Quantity	Total cost (Rs)
Materials				
Glass Cover	Transparent cover for solar still	850	1	850
Basin Material	Material for the basin (G.I. sheet)	1800	1	1800
Insulation	Insulating material for heat retention	115	1	115
Thermocouple	Fix at various points to read the temperature	100	12	1200
12-Point Indicator	Digital metre to note the temperature at different points	2300	1	2300
Sealants and Adhesives	To ensure airtight assembly	175	2	350
Wicks (Bamboo Cotton)	Material for enhancing water absorption	1	1 Bundle	1000
Measuring jar	Measure exact output	25	1	25
Fabrication and installation				
Labour & fabrication	Cost of assembling and installing the still	1500	1	1500
Operational costs				
Maintenance	Annual maintenance cost	500	1/year	500/year
Total initial cost				9,340.00
Total annual cost	Including maintenance			500/year
Productivity and cost per litre				
Daily productivity	Amount of distilled water produced per day		2330 mL/day (4.66 L/m^2/day)	
Annual productivity	Assuming 365 days of operation		495 L/year	
Cost per litre (0.5m^2 Area)	Initial cost spread over the first year.			(9340 + 500) / 495 = Rs. 19.88/L

scenario (Rs. 4.46/L), which remains below the retail packaged water price threshold. These findings are encouraging enough to make the optimised single-slope solar still a practical option for decentralised household water production in water-scarce and energy-poor communities.

6. Conclusion

A single-slope solar still with different wall lining thicknesses was fabricated and tested experimentally. The effects of ambient temperature, wall lining thickness, solar radiation, and wind velocity on freshwater productivity were optimised using RSM based on Central Composite Design. Experimental results confirmed that all selected parameters significantly affected freshwater production. The obtained significant results from both experimental and statistical analysis are listed below.

(1) The maximum temperature recorded in the basin (T_b), glass (T_g), water (T_w) and vapour (T_v) was 68.5°C, 63.25°C, 68°C and 66.5°C respectively. The 8 mm wall lining configuration had the highest Tw and Tb for all test hours, which corresponds to the largest vapour-to-glass temperature difference (Tv – Tg) and the highest condensation rate and distillate yield of the three wall lining configurations tested.
(2) Freshwater productivity increased from 1260 mL/day (2.52 L/m^2/day) for the unlined still to 2230 mL/day (4.46 L/m^2/day) and 2330 mL/day (4.66 L/m^2/day) for 4 mm and 8 mm wall lining thicknesses, respectively. The optimised 8 mm cotton cloth lining achieved an overall productivity improvement of 85% compared with the conventional still using a low-cost modification below Rs. 1,000.
(3) The developed RSM model showed high prediction accuracy with $R^2 = 0.9926$, Adjusted $R^2 = 0.9857$, and Predicted $R^2 = 0.9595$, indicating good agreement between experimental and predicted results without overfitting. Model validation under optimised conditions produced an experimental yield of 2330 mL/day with only 1.96% prediction error.
(4) Solar radiation was the dominant parameter affecting freshwater productivity ($F = 1910.85$, $p < 0.0001$), followed by the interaction between wall lining thickness and solar radiation ($F = 18.58$, $p = 0.0006$). Wind velocity improved condensation by cooling the glass cover, and within the tested range of 1–2 m/s, this effect enhanced freshwater productivity.
(5) The optimum operating conditions within the investigated range were 40°C ambient temperature, 8 mm wall lining thickness, 900 W/m^2 solar radiation, and 2 m/s wind velocity, producing an experimental freshwater yield of 2330 mL/day with a prediction error of 1.96%. The estimated long-term freshwater production cost was approximately Rs. 2.89/L, with a payback period of about 2.5–4 years, indicating good economic feasibility for decentralised applications.
(6) The distilled water satisfied WHO (2017) drinking water standards with TDS of 12 ± 3 ppm, pH 6.9 ± 0.1, electrical conductivity of 22 ± 5 μS/cm, and turbidity below 0.5 NTU. The study demonstrated that optimising cotton cloth wall lining thickness within the RSM-CCD framework improved freshwater productivity by 85% using a low-cost modification below Rs. 1,000.

6.1. Limitations

Despite the promising results, the methods used in this study have several limitations. Advanced materials such as multiwall carbon nanotubes (MWCNTs) and specialised coatings can be costly and may not be readily available, hindering scalability and commercial viability. The fabrication techniques like sand-blasting, milling, and shot-blast aided corrugation require specialised equipment and expertise, which may not be feasible for widespread or rural applications. Long-term durability and maintenance of nanofluid-based and modified solar stills need further investigation, as issues like material degradation, fouling, or clogging could impact performance over time. Additionally, the environmental impact of producing and disposing of advanced materials used in the nanofluids and coatings requires assessment. The identified optimum conditions may be specific to the experimental setup and local environmental conditions, and replicating these in different climates or with different water sources may yield varying results. Finally, scaling up the system from controlled experimental conditions to real-world applications may present unforeseen challenges in terms of efficiency, cost, and practicality. Addressing these limitations in future research will be crucial for advancing the practical application of enhanced solar still technologies.

6.2. Future scope

Future research should focus on advanced material investigations, such as exploring different nanofluids and composite materials to enhance thermal and electrical conductivity further and studying the long-term durability and stability of these materials in solar still applications. Additionally, integrating phase change materials (PCMs) could provide better thermal energy storage and release. Optimising geometric configurations of solar stills is another area for future study, including evaluating different angles and shapes to maximise surface area for condensation and improve sunlight absorption. Moreover, incorporating additional heat transfer mechanisms, such as fins or heat exchangers, could significantly enhance the efficiency of solar stills. Finally, exploring automation and control systems for regulating temperature and water levels could lead to more efficient and user-friendly solar still designs.

Future research should also explore the integration of hybrid solar still systems, combining photovoltaic panels with thermal collectors to simultaneously generate electricity and distilled water. Investigating the impact of varying environmental conditions, such as humidity and dust accumulation, on the performance of solar stills is essential. Additionally, the development of cost-effective and scalable fabrication techniques for advanced materials will be crucial for widespread adoption. Implementing real-time monitoring and data analytics can optimise operational parameters and improve efficiency. Collaboration with industry partners can accelerate the transition from laboratory research to commercial applications. Finally, conducting life cycle assessments will provide insights into the environmental and economic sustainability of advanced solar still designs.

Author contributions

CRediT: **T. G. Sakthivel:** Data curation; **R. Manikandan:** Formal analysis, Writing – original draft; **S. Purushothaman:** Supervision; **N. Punitha:** Investigation; **T. Gopalakrishnan:** Methodology; **C. Gnanavel:** Project administration, Validation, Visualization; **V. S. Shaisundaram:** Conceptualization, Writing – review & editing

Disclosure statement

No potential conflict of interest was reported by the author(s). During the preparation of this work, the author(s) utilised Grammarly solely for language refinement and grammar correction. No generative AI tools were involved in the development of scientific content, data interpretation, or any core research processes.

Data availability statement

The data that support the findings of this study are openly available in Zenodo at DOI: 10.5281/zenodo.21379030.

ORCID

T. G. Sakthivel http://orcid.org/0000-0002-0811-7065
R. Manikandan http://orcid.org/0000-0002-6158-2599
S. Purushothaman http://orcid.org/0000-0002-1427-1851
N. Punitha http://orcid.org/0000-0002-4496-1669
T. Gopalakrishnan http://orcid.org/0000-0003-0923-4076
C. Gnanavel http://orcid.org/0000-0002-1242-851X

References

Abed, F. M., A. H. Ahmed, M. Hasanuzzaman, L. Kumar, and N. M. Hamaad. 2022. "Experimental Investigation on the Effect of Using Chemical Dyes on the Performance of Single-Slope Passive Solar Still." *Solar Energy* 233:71–83. https://doi.org/10.1016/j.solener.2021.12.060

Ahmed, H. M. 2016. "The Effects of Various Types and Layouts of Wick Materials on the Thermal Performance of Conventional Solar Stills." In: *Proceedings of the 4th IEEE International Conference on Smart Energy Grid Engineering*, 84–89.

Bhargva, M., and A. Yadav. 2019. "Experimental Investigation of Single Slope Solar Still Using Different Wick Materials: A Comparative Study." *Journal of Physics: Conference Series* 1276 (1): 012042. https://doi.org/10.1088/1742-6596/1276/1/012042.

Durkaieswaran, P., and K. K. Murugavel. 2015. "Various Special Designs of Single Basin Passive Solar Still: A Review." *Renewable & Sustainable Energy Reviews* 49:1048–1060. https://doi.org/10.1016/j.rser.2015.04.111

El Hafid, W., S. Abderafi, K. Amghar, et al. 2023. "Modeling and Design of a New System Cascade Solar Still Test for Thermal Performance." *International Journal of Energy and Environmental Engineering* 14 (3): 549–562. https://doi.org/10.1007/s40095-022-00534-0.

Garg, H. P. 1975. "Effect of Climatic, Operational and Design Parameters on the Year-Round Performance of Single-Sloped and Double-Sloped Solar Still under Indian Arid Zone Conditions." *Solar Energy* 17:159–177.

Haitham, O., M. Jamel, and S. Ihab. 2020. "Statistical Analysis and Mathematical Modeling of Modified Single Slope Solar Still." *Energy Sources Part A Recovery, Utilization and Environmental Effects* 43 (21): 1–19.

Hanshik, C., H. Jeong, K. Jeong, and S. Choi. 2016. "Improved Productivity of the MSF Desalination Plant by Increasing the Top Brine Temperature." *Energy* 107:683–692. https://doi.org/10.1016/j.energy.2016.04.028

Hussen, H. M., M. M. Younes, W. H. Alawee, A. S. Abdullah, S. A. Mohammed, T. E. M. Atteya, F. Abbas, and Z. M. Omara. 2023. "An Experimental Comparison Study Between Four Different Designs of Solar Stills." *Case Studies in Thermal Engineering* 44:102841. https://doi.org/10.1016/j.csite.2023.102841

Kabeel, A. E., and M. Abdelgaied. 2016. "Improving the Performance of Solar Still by Using PCM as a Thermal Storage Medium under Egyptian Conditions." *Desalination* 383: 22–28. https://doi.org/10.1016/j.desal.2016.01.006.

Kabeel, A. E., S. W. Sharshir, G. B. Abdelaziz, M. A. Halim, and A. Swidan. 2019. "Improving Performance of Tubular Solar Still by Controlling the Water Depth and Cover Cooling." *Journal of Cleaner Production* 233: 848–856. https://doi.org/10.1016/j.jclepro.2019.06.104.

Keshtkar, M., M. Eslami, and K. Jafarpur. 2020. "Effect of Design Parameters on Performance of Passive Basin Solar Stills considering Instantaneous Ambient Conditions: A Transient CFD Modeling." *Solar Energy* 201:884–907. https://doi.org/10.1016/j.solener.2020.03.068

Lauer, L., L. Marder, T. Benvenuti, and A. Moura. 2019. "Electrodialysis Applied to the Treatment of University Sewage for Water Recovery." *Journal of Environmental Chemical Engineering* 7:102982. https://doi.org/10.1016/j.jece.2019.102982

Liu, J., Q. Wang, H. Shan, H. Guo, and B. Li. 2019. "Surface Hydrophobicity-Based Heat and Mass Transfer Mechanism in Membrane Distillation." *Journal of Membrane Science* 580: 275–288.

Nafey, A. S., M. Abdelkader, A. Abdelmotalip, and A. A. Mabrouk. 2000. "Parameters Affecting Solar Still Productivity." *Energy Conversation*

and Management 41 (16): 1797–1809. https://doi.org/10.1016/S0196-8904(99)
00188-0.

Qasim, M., M. Badrelzaman, N. N. Darwish, and N. A. Darwish. 2019. "Reverse Osmosis Desalination: A State-of-the-Art Review." *Desalination* 459:59–104. https://doi.org/10.1016/j.desal.2019.02.008

Rejeb, O., M. S. Yousef, C. Ghenai, H. Hassan, and M. Bettayeb. 2021. "Investigation of Solar Still Behaviour Using Response Surface Methodology." *Case Studies in Thermal Engineering* 24:100816. https://doi.org/10.1016/j.csite.2020.100816

Senthilkumar, N., M. Yuvaperiyasamy, and B. Deepanraj. 2024. "Application of Taguchi Design to Optimize the Operational Parameters of Pyramid Solar Still Integrated with TiO_2 Nanoparticles." *Engineering Research Express* 6 (4): 045540. https://doi.org/10.1088/2631-8695/ad8b0f

Srivastava, P., and S. Agrawal. 2013. "Winter and Summer Performance of Single Sloped Basin Type Solar Still Integrated with Extended Porous Fins." *Desalination* 319:73–78. https://doi.org/10.1016/j.desal.2013.03.030

Suraparaju, S. K., and S. K. Natarajan. 2020. "Performance Analysis of Single Slope Solar Desalination Setup with Natural Fiber." *Desalination and Water Treatment* 193:64–71. https://doi.org/10.5004/dwt.2020.25679

Suraparaju, S. K., and S. K. Natarajan. 2021. "Experimental Investigation of Single-Basin Solar Still Using Solid Staggered Fins Inserted in Paraffin Wax PCM Bed for Enhancing Productivity." *Environmental Science and Pollution Research* 28: 20330–20343. https://doi.org/10.1007/s11356-020-11980-w.

World Health Organization (WHO). 2017. *Guidelines for Drinking-water Quality*. 4th ed., incorporating the first addendum. Geneva: World Health Organization.

Yuvaperiyasamy, M. 2025. "Experimental Investigation Focuses on the Desalination Productivity and Water Quality Using a Nano CuO-Coated Floated Absorber in a Solar Still." *Turkish Journal of Engineering* 9 (4): 791–800. https://doi.org/10.31127/tuje.1638403

Yuvaperiyasamy, M., S. Kumaravel, K. Sabari, and M. Kalaimani. 2025. "Optimization of Single-Slope Solar Still with Different Energy Storage Materials Using the Taguchi and Machine Learning Methods." *Results in Engineering* 27:106809. https://doi.org/10.1016/j.rineng.2025.106809

Yuvaperiyasamy, M., N. Senthilkumar, and B. Deepanraj. 2025. "Enhancing Pyramid Solar Still Performance through Varied Heat Storage Materials and Water Depths: A Comprehensive Experimental Study." *Recent Patents on Mechanical Engineering* 18 (2): 148–157. https://doi.org/10.2174/0122127976288061240228045000